Picosecond Energy Transfer at Gold/Electrolyte Interfaces Using Transient Reflecting Grating Method under Surface Plasmon Resonance Condition

Kenji Katayama, Tsuguo Sawada,* Isao Tsuyumoto,† and Akira Harata††

Department of Advanced Materials Science, Graduate School of Frontier Sciences, The University of Tokyo, 7-3-1 Hongo, Bunkyo-ku, Tokyo 113-8656

†Department of Environmental Systems Engineering, Kanazawa Institute of Technology, 7-1 Ohgigaoka, Nonoichi, Ishikawa 921-8501

††Department of Molecular Science and Technology, Graduate School of Engineering Science, Kyushu University, 6-1 Kasugakoen, Kasuga, Fukuoka 816-8580

(Received March 3, 1999)

The energy transfer dynamics at gold/NaCl aq (0—0.5 M) interfaces was investigated using our recently developed surface plasmon resonance transient reflecting grating (SPR-TRG) method. We focused on two exponential decays in the SPR-TRG signals. The two decays correspond to the relaxation of hot electrons and interfacial heat transfer, respectively. The intensity of each decay changes systematically with increases in the concentration of NaCl, i.e., the former becomes smaller and the latter becomes larger. Considering the relation between the intensity and the dynamics, we concluded that there is some interaction between the hot electrons and the adsorbate on the interface and that the following temperature rise in gold after relaxation of the hot electrons becomes large. This conclusion shows that an ultrafast energy transfer processes by hot electrons exists, and that the process is hindered by the adsorbate. Finally, we discuss the ultrafast energy transfer in relation to the hot electrons and adsorbate on a molecular scale.

Information on energy transfer at a solid–liquid interface is useful to clarify various processes occurring in electrochemical and catalytic reactions. However, the fundamental processes of ultrafast energy transfer on a time scale from femtoseconds to nanoseconds are still unclear. The energy transfer processes at a nanometer scale interfacial region involve complicated interactions, such as electron–phonon and phonon–phonon interactions between solid, liquid, and adsorbed species. When a metal/liquid interface is irradiated by light, the energy is at first stored as temperature rise of the electrons in the metal. Within several picoseconds, the temperature becomes higher than that of the phonons.[1] We call such electrons in a non-equilibrium state hot electrons here. After relaxation of the hot electrons, the energy is converted into a temperature rise of the metal, itself. According to the conventional concept of thermal conduction, the temperature falls on a time scale of nanoseconds through thermal conduction from the metal to the liquid.[2] On this time scale, a phonon–phonon interaction is mainly involved in the energy transfer between the metal and the liquid, because the relaxation process of hot electrons has already been completed. On the other hand, recent studies with femtosecond pulsed-lasers suggest an ultrafast electronic interaction between hot electrons and adsorbed ions in the energy-transfer processes.[3,4]

In order to clarify the energy-transfer processes at the solid–liquid interface, in situ measurements with an ultrafast time resolution are necessary, but most reported methods require a vacuum condition. For this reason, only a few techniques have been applied to solid–liquid interfaces,[3—7] unlike the case with solid surfaces.[8—13] Transient reflection (TR) and transient reflecting grating (TRG) methods can be applied to dynamics measurements at solid–liquid interfaces.[3—5] The TR method with a time resolution of 200 fs has been applied to elucidate the interaction between adsorbed hydrogen ions and hot electrons at an electrochemically controlled platinum/electrolyte interface.[3] The same method was used to study interfaces between platinum/various electrolytes, and a 20 fs interaction was found between various adsorbed anions and nonthermalized electrons at the interfaces.[4] In addition to these femtosecond studies, the TRG method with a time resolution of 80 ps has been applied to investigate elastic deformation caused by heat generation at an electrochemically controlled interface.[5] The results have suggested that the adsorbate played an important role in energy transfer.

The TR and TRG methods have some disadvantages regarding detection capability. The TR method cannot detect a reflectivity change smaller than 10^{-6}. The reflectivity change due to the relaxation of hot electrons on a picoseconds time scale is about 10^{-4}, but that due to thermal diffusion on a nanoseconds time scale is only 10^{-6}, thus, detection with an adequate S/N ratio is difficult to achieve. The TRG method

cannot detect thermal diffusion selectively for two reasons. One is that thermal diffusion cannot be directly detected because the information on thermal diffusion is deduced from an analysis of the surface deformation due to thermal expansion. The other is that thermal diffusion and the surface acoustic wave components are mixed in the signal.[14]

We have newly developed a surface plasmon resonance (SPR) TRG method.[15] By utilizing the SPR condition, we could successfully enhance the signal intensity due to a refractive index change. The signal of thermal diffusion on a nanoseconds time scale can be detected with a 20-times larger intensity, and that of the hot electrons on a picoseconds time scale can be also selectively detected with a 100-times larger intensity, compared to the conventional TRG method.[16]

In this study we applied the SPR-TRG technique to solid–liquid interfaces, while utilizing the advantages that both picosecond electronic interactions and nanosecond thermal energy transfer can be directly detected in situ with high sensitivity. Our purpose in this study was to clarify the energy transfer processes involving adsorbed ions at metal/solution interfaces on a wide time scale from picoseconds to nanoseconds by measurements of gold/NaCl aq solution interfaces. We looked at how the quantity of adsorbed species affects the electronic interactions and thermal energy transfer processes. Based on the results, we propose a model for the initial energy transfer processes at a solid/liquid interface.

1. Experimental

The SPR-TRG experimental setup was the same as previously reported.[14] Only a brief outline follows here. A mode-locked Q-switched Nd : YAG laser (Quatronix, model 416) was used as a light source, and the frequency was doubled using a nonlinear optical crystal. The pulse train wavelength was 532 nm with a repetition rate of 1 kHz and a pulse width of 80 ps in full width at half maximum. The pulse was separated into pump and probe pulses using a partial reflective mirror. The pump beam was further divided into two beams by a half mirror. The two pump pulses were crossed and irradiated onto the same spot of the sample surface so as to coincide in time to form an interference pattern. The probe pulse was irradiated at the center of the spot after passing through a computer-controlled optical delay line. The reflecting diffracted light was monitored with a photomultiplier (PMT) connected to a flexible light guide, whose entrance was placed at one of the first order reflecting diffraction spots. The output signal from the PMT was gated and averaged over one millisecond with a boxcar integrator before an analog-to-digital transformation for computer storage. The spot diameters of the pump and probe beams were 60 and 40 μm, respectively.

The sample was a gold film (thickness: 40 nm) vapor deposited on the surface of a hemicylindrical glass prism (LaSF15, refractive index: 1.89 at 532 nm). The Kretschmann configuration was employed as the sample arrangement for the SP resonance (Fig. 1(a)). Two pump pulses and one probe pulse were incident from the prism side onto the gold film. The sample was loaded on a rotary stage to allow the incident angle of the laser beams to be changed. The incident angle was fixed to the SP resonance angle, which was larger than the total reflectional angle. The SP was excited only by the p-polarized light, and was thus controlled by changing the

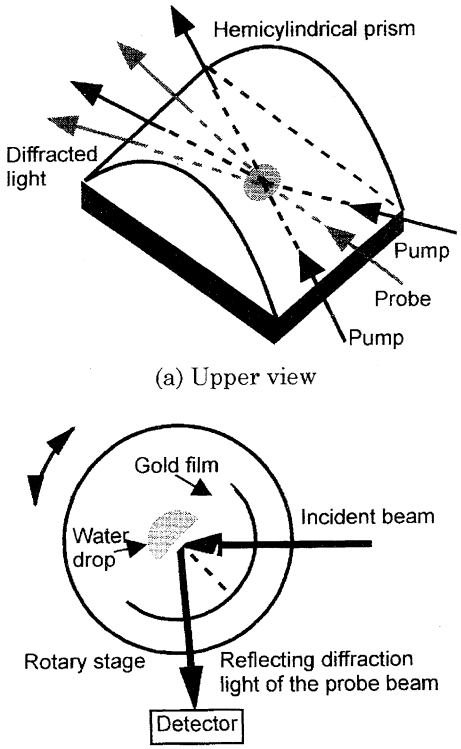

Fig. 1. Schematic illustrations of the arrangement of the sample and laser beams. The two pump beams overlapped and formed an interference fringe pattern on the gold film/prism interface. The generated transient grating was detected by the reflecting diffraction of the probe beam. The incident angle was kept to the surface plasmon angle, 54 degrees. The gold/solution interface was prepared using a drop of NaCl aqueous solution at the focused point.

polarization of the pump and the probe beams with two half-wave plates.

In a TRG measurement, the spatially modulated physical change due to excitation by a pulsed optical interference fringe is measured by the diffraction of the probe light. When the probe light is under a SP resonance, a refractive index change can be detected with high enhancement.[15] For gold, when both the pump and probe beams are under a SP resonance condition, the relaxation signal of hot electrons induced by SP within several picoseconds can be detected with 100 times larger intensity than for the conventional TRG method.[16] The picoseconds exponential decay signal is observed after being transformed into a convoluted waveform with an incident pulse whose duration is 80 ps. When only the probe light is under the SPR condition, no signal for the hot electrons is detected. Only the temperature rise after relaxation of the hot electrons and the following thermal diffusion is detected with 20 times larger intensity than that obtained with the conventional TRG method.[15]

For the experiments, the SPR angle (SP angle) should be determined. The angle was estimated by the Fresnel theory. The reflectivity, calculated as a function of the incident angle, has a minimum at the SP angle, because most of the incident light energy is converted into SP energy. We calculated the SP angle for the LaSF15/gold (40 nm)/water structure as being 54 deg. The refractive indexes (at 532 nm) for LaSF15, gold and water used in this calculation were 1.89, 0.402+2.45i, and 1.33, respectively.[17]

Furthermore, we experimentally confirmed the SP angle as being 54 deg by detecting the reflectivity minimum while scanning the incident angle.

We prepared the metal/water interface as shown in Fig. 1(b) using a drop of NaCl aqueous solution at the focusing point. The concentrations of NaCl aq were 0, 0.01, 0.1, 0.25, 0.5 M (1 M = 1 mol dm^{-3}). The solutions were prepared with NaCl (Kanto Chemical, 99.5%) and purified water from a Millipore Milli-xq system. While a transient waveform was being measured, the solution did not become dry.

The experiments were carried out under two conditions: The SPR condition for both the pump and probe beams and, for only the probe beam. Under the latter condition, the intensities of the pump and probe beams were 100 and 10 nJ/pulse, respectively, but in the former condition they were 20 and 10 nJ/pulse, respectively, so as not to damage the sample due to SP excitation. When only the probe beam was used under the SP condition, a polarizing plate was inserted in front of the detector to obtain detection of only the polarized component of the probe beam. The overall signal fluctuation during the measurement was estimated to be less than 5%. The grating spacing was maintained at 2.14 μm throughout the experiments.

2. Data Analysis

TRG signals can be analyzed with the following equation:[18]

$$S_{TRG}(t) = A(g(t))^2, \tag{1}$$

where S_{TRG} is the intensity of the TRG signal, A is a constant determined by the sensitivity of the equipment and $g(t)$ is a function of time which represents the physical property change of a sample.

For measurements with SPR of both the pump and probe beams, two relaxation components are observed for a sample of gold.[16] The faster component is the relaxation of hot electrons on a time scale of several picoseconds, which is much shorter than the pulse duration used in our experiment. The slower component is the temperature fall of gold due to thermal diffusion on a time scale of several nanoseconds. Then,

$$g(t) = A_1 \cdot \exp\left(-\frac{t}{\tau_e}\right) + A_2 \cdot \left(a_1 \cdot \exp\left(-\frac{t}{\tau_{para}}\right) + (1-a_1) \cdot \exp\left(-\frac{t}{\tau_{vert}}\right)\right), \tag{2}$$

where A_1, A_2, and a_1 are constants, τ_e is the relaxation time of the hot electrons, τ_{para} is the time which lapses until the holographic temperature distribution disappears due to thermal diffusion parallel to the interface, and τ_{vert} is the time for the temperature fall due to thermal transfer through the interface. The thermal diffusion component may seem to have a single exponential decay with the relaxation time τ ($1/\tau = 1/\tau_{para} + 1/\tau_{vert}$), but this is not true. Under our experimental condition, the relaxation time due to parallel thermal diffusion is faster than that due to the interfacial thermal transfer. Nevertheless, the holographic temperature distribution still does not disappear at the time of τ_{para}. This is because boundary conditions must be satisfied, although the temperature at the water side does not change as rapidly as gold due to the low thermal conductivity of water. The remaining temperature distribution disappears due to interfacial thermal transfer. Thus, the overall thermal relaxations are expressed by a double exponential decay. τ_{para} is determined by the thermal property of only gold, because the holographic temperature distribution is made only in the gold and then the thermal diffusion parallel to the interface occurs only there. Then, τ_{para} can be theoretically obtained from the thermal diffusion equation. τ_{para} is the time during which heat diffuses for the length of the grating spacing, and is calculated as[14]

$$\frac{1}{\tau_{para}} = D\left(\frac{2\pi}{\Lambda}\right)^2, \tag{3}$$

where D is the thermal diffusion coefficient of gold and Λ is the grating spacing.

For measurements with SPR of only the probe beam, only the temperature rise and the following fall due to thermal diffusion are observed. In this case, the second component in Eq. 2 is detected. Thus $g(t)$ is expressed as

$$g(t) = A_2' \cdot \left(a_1 \cdot \exp\left(-\frac{t}{\tau_{para}}\right) + (1-a_1) \cdot \exp\left(-\frac{t}{\tau_{vert}}\right)\right), \tag{4}$$

where A_2' is a constant.

For measurements at gold/aqueous solutions, the TRG signals include some oscillations in addition to the components in Eqs. 2 and 4 in both cases of measurements with SPR of both the pump and probe beams and of only the probe beam. In these cases, Eqs. 2 and 4 are revised as

$$g(t) = A_1 \cdot \exp\left(-\frac{t}{\tau_e}\right) + A_2 \cdot \left(a_1 \cdot \exp\left(-\frac{t}{\tau_{para}}\right) + (1-a_1) \cdot \exp\left(-\frac{t}{\tau_{vert}}\right)\right) + A_3 \cos(2\pi F t) \exp\left(-\frac{t}{\tau_a}\right), \tag{5}$$

$$g(t) = A_2' \cdot \left(a_1 \cdot \exp\left(-\frac{t}{\tau_{para}}\right) + (1-a_1) \cdot \exp\left(-\frac{t}{\tau_{vert}}\right)\right) + A_3' \cos(2\pi F t) \exp\left(-\frac{t}{\tau_a}\right), \tag{6}$$

where A_3 is a constant, F is the acoustic frequency, and τ_a is the attenuation time of the acoustic wave.[18]

We neglected the acoustic term for analysis because the measured TRG signals have too small A_3 and A_3' components to fit the acoustic term with Eqs. 5 and 6. Thus, we used Eqs. 2 and 4 thoughout this analysis. In the case of fitting the signals with SPR of both the pump and probe beams, we used the convolution of the $g(t)$ in Eq. 2 with the incident pulse as a fitting function, because τ_e is much smaller than the pulse duration. While the fitting accuracy should be within a picosecond to obtain the relaxation time of hot electrons, the accuracy of the fitting above is, in fact, over 10 ps. As a countermeasure, we kept τ_e equal to the literature value, 5 ps in the fitting above.[2] As a result, the obtained A_1 value is influenced by the change of the convoluted peak value when the τ_e value changes.

To summarize the fitting procedure, first, τ_{para} was theoretically obtained from Eq. 3, and was 0.89 ns using $\Lambda = 2.14$

μm and $D = 1.30\ \mathrm{cm^2\ s^{-1}}$. Secondly, the signal with SPR of only the probe beam was fitted with Eq. 4 to obtain the values of A_2', a_1, and τ_{vert}. Finally, the signal with SPR of both the pump and probe beams was fitted by the above-mentioned method to obtain the values of A_1 and A_2. In this study, we focused on the values of A_1 and A_2', which are the signal intensities of hot electrons and temperature rise components, respectively. While there is no difference between the physical meanings of A_2 and A_2', we used A_2' because the overlap of the A_1 and A_2 components made it difficult to obtain A_2 exactly.

Finally, we clarify the physical meanings of the A_1 and A_2' changes. The A_1 value is proportional to the refractive index change due to photoexcited hot electrons. When the hot electrons are excited or relaxed to a physically different state, the refractive index change is varied, and thus the A_1 value is changed. Furthermore, there is another factor which changes the A_1 value. The relaxation time of the hot electrons is much shorter than the pulse duration and, as a result, a small change of the relaxation time influences the A_1 value through convolution, as stated in the previous paragraph. The A_2 value is proportional to the refractive index change due to the maximum temperature rise of gold. The refractive index change is proportional to temperature rise within the range of our experimentally obtained temperature, which is estimated to be less than 50 K. Therefore the A_2 value is proportional to the maximum temperature rise. The temperature rise is caused by heat generated in the relaxation process of the hot electrons. In our experiments, we did not have sufficient time resolution to separate each component of the hot electrons and the temperature rise, but we successfully detected each component selectively using our unique methods with SPR of both the pump and probe beams and of only the probe beam.

3. Results and Discussion

The transient waveforms for the gold/water and gold/air interfaces are shown in Fig. 2. Figures 2(a) and 2(b) are the detected signals under the SP condition of both the pump and probe beams, and of only the probe beam, respectively. The signals for the gold/water and gold/air interfaces were measured under the same conditions of laser intensity, detector sensitivity and optics alignment. The detected waveforms in Fig. 2(a) include sharp peaks appearing at the same time as the pulse duration, followed by an exponential decay of the relaxation time, 1 ns for the gold/air interface and more than 5 ns for the gold/water interface. The exponential decay for the gold/water interface also includes some oscillations. The waveforms in (b) have almost the same shape as in (a), except for the peak at time zero.

As we previously reported,[16] the peak around time zero shown in Fig. 2(a) is due to the refractive index change by hot electrons induced by SP. We cannot compare the peak intensities at the gold/air and the gold/water interfaces because of the difference in the signal enhancement factor for the SP resonance of each interface. The subsequent relaxation after the peak in Fig. 2(a) and the exponential decay

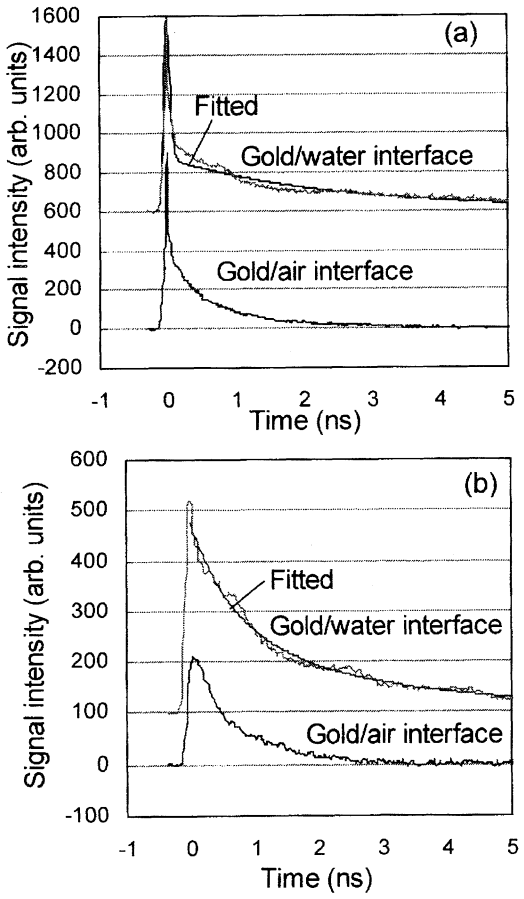

Fig. 2. Transient reflecting grating responses for the gold (40 nm)/air and gold (40 nm)/water interface when both the pump and probe beams were under the surface plasmon resonance condition (a) and when only the probe beam is under the surface plasmon resonance condition (b). In both (a) and (b), the waveforms for the gold/water interface are vertically displaced for clarity. The fitted curves were also shown for the signals at the gold/water interface.

in Fig. 2(b) are due to thermal diffusion. While the thermal diffusion time for the gold/air interface was 1 ns, that for the gold/water interface was much longer. As mentioned in Section 2, the thermal diffusion is divided into two types according to the direction, that is, parallel and perpendicular to the interface. With regard to the parallel diffusion, there is no difference between the gold/air and gold/water interfaces, as explained in Section 2. Therefore, the difference in the relaxation time between the two interfaces is regarded as being due to the difference in the perpendicular thermal transfer. In conventional TRG experiments, oscillations like those shown in Figs. 3(a) and 3(b) have been regarded as signals due to surface displacement perpendicular to the interface by the surface acoustic wave.[14] However, we have found that only the refractive index change can be selectively detected at the SP resonance angle. Considering the fact that the oscillations were detected only for a solid–liquid interface, we attributed them to acoustic waves in the liquid phase near to the interface generated by the holographic thermal conduction from solid to liquid.[5] We estimated that

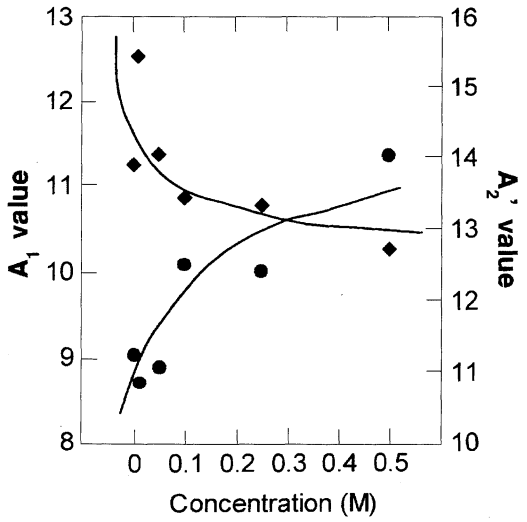

Fig. 3. The dependence of the A_1 (◆) and A_2' (●) values on the NaCl concentration. The tendencies of A_1 and A_2' are shown with smooth lines. A_1 and A_2' are fitting parameters for the transient reflecting grating signals with SPR of both pump and probe beams and only the probe beam respectively. The detailed meanings are explained in the Section 2.

the wave is localized approximately within 20 nm from the interface because the thermal diffusion length for 5 ns is calculated to be 17 nm. An acoustic wave close to the interface induces a density change of the liquid, that is, a refractive index change.

Next, we examined how the energy transfer processes at the solid–liquid interface are influenced by adsorbed ions. The transient responses at gold/NaCl (0—0.5 M) were measured by the two techniques. We selected chloride ions because of their easy adsorption on gold.[19—21] The transient waveforms show a systematic change with increasing NaCl concentration. We fitted all of the waveforms by the method explained in Section 2. The signals at any concentration could be fitted using $\tau_{para} = 0.89$ ns, $\tau_{vert} = 6$ ns. Example-fitted signals at the gold/solutions interfaces are shown in Fig. 2. We investigated the dependence of the A_1 and A_2' values on the NaCl concentration and show this in Fig. 3. With increasing concentration, A_1 decreases and A_2' increases.

It is difficult to clarify the physical meaning for the A_1 decrease, because the variation in the refractive index change has two causes, as explained earlier. Nevertheless, we can say that the adsorbed ions have some influence on the excitation or relaxation processes of not electrons. Next, we considered the A_2 increase. A_2 is proportional to the temperature rise of gold. The temperature rise originates in the heat generated in the relaxation process of the hot electrons. Then, this result indicates that the generated heat increases with increasing number of adsorbed ions. However, the generated heat cannot increase because no absorption change of the sample was detected. This contradiction can be explained only if we can consider an ultrafast interfacial energy transfer before relaxation of the hot electrons. Our assumption is as follows: Although the hot electrons originally impart some energy to the liquid molecules, an interruption of the process due to the adsorbed ions results in increased heat generation in the gold. This concept is supported by the A_1 result, which suggests an interaction between the hot electrons and adsorbed ions.[16] In brief, there are energy transfer processes from the hot electrons of gold to water molecules, competing with the heat generation in gold. The fast interfacial energy tramsfer is hindered by the adsorption of chloride ions.

We considered what these results reflect fundamental processes on a molecular scale. In electrochemistry, the electronic distribution in a metal is often expressed by a jellium model,[22] where the density of electrons decreases exponentially while moving away from the interface. During the excitation and relaxation of electrons, the density distribution of electrons would vary and would generate local and transient polarizations. We assume that the initial energy transfer is caused by an interaction between the polarizations and the dipole moment of the water molecules. We next considered how the adsorbed ions affect the initial energy transfer. Adsorbed ions are generally solvated by some water molecules, even at the interface,[22—24] which are oriented towards the ions by the ion–dipole interaction. We assume that the transient polarization is screened by the oriented water molecules, and that the initial energy transfer is hindered.

Concerning the origin of the polarization of a metal, we can suppose two kinds of excited states of electrons, nonthermalized electrons and hot electrons. The former are electrons which do not obey the Fermi distribution within several hundred femtoseconds.[8,23] The latter are electrons prior to thermal equilibrium, whose temperature is still higher than that of phonons.[2,24] Some recent papers have suggested energy transfer by nonthermalized electrons.[3,4] It should be possible to differentiate the two processes with a better time resolution. The SPR-TRG method with femtosecond time resolution should make these things clearer.

4. Conclusions

We applied the SPR-TRG method to energy transfer dynamics measurements at gold/NaCl aq (0—0.5 M) interfaces. We found that the dynamics of hot electrons in gold on a picoseconds time scale showed a systematic change; also the following temperature rise in gold became larger with increasing concentration of the solution. From these results, we determined that the energy transfer processes due to hot electrons occurred between the gold and water, and that the processes were hindered by the adsorbed ions. We assumed that the energy transfer occurred by way of interactions between water molecules and transient local polarization of hot electrons at the interface. The hindrance of the energy transfer by adsorbed ions was assumed to be due to a screening of the transient local polarization by the water molecules oriented to the ions.

This work was supported by Grant-in-Aids for Specially Promoted Research (No.07102004) and for Scientific Research on Priority Area of Electrochemistry of Ordered Interfaces (No.09237219) from the Ministry of Education, Sci-

ence, Sports and Culture.

References

1 Q. Shen, A. Harata, and T. Sawada, *Jpn. J. Appl. Phys.*, **35**, 2339 (1996).

2 C. K. Sun, F. Vallee, L. H. Acioli, E. P. Ippen, and J. G. Fujimoto, *Phys. Rev. B*, **50**, 15337 (1994).

3 A. Harata, T. Edo, and T. Sawada, *Chem. Phys. Lett.*, **249**, 112 (1996).

4 A. Hibara, A. Harata, and T. Sawada, *Chem. Phys. Lett.*, **272**, 1 (1997).

5 A. Harata, T. Kawasaki, M. Ito, and T. Sawada, *Anal. Chim. Acta*, **299**, 349 (1995).

6 L. A. Gomez-Jahn and R. J. D. Miller, *J. Chem. Phys.*, **96**, 3981 (1992).

7 J. J. Kasinski, L. A. Gomez-Jahn, K. J. Faran, S. M. Gracewsk, and R. J. D. Miller, *J. Chem. Phys.*, **90**, 1253 (1989).

8 R. H. M. Groeneveld, R. Sprik, and A. Lagendijk, *Phys. Rev. B*, **51**, 11433 (1995).

9 A. H. Zewail, *J. Phys. Chem.*, **100**, 12701 (1996).

10 W. Ho, *J. Phys. Chem.*, **100**, 13050 (1996).

11 S. Ogawa and H. Petek, *Surf. Sci.*, **357-358**, 585 (1996).

12 A. Aeschlimann, M. Bauer, and S. Paulik, *Chem. Phys.*, **205**, 127 (1996).

13 R. W. Schoenlein, J. G. Fujimoto, G. L. Eesley, and T. W. Capehart, *Phys. Rev. B*, **43**, 4688 (1991).

14 A. Harata and T. Sawada, *Trends Anal. Chem.*, **14**, 504 (1995).

15 K. Katayama, Q. Shen, A. Harata, and T. Sawada, *Appl. Phys. Lett.*, **69**, 2468 (1996).

16 K. Katayama, Q. Shen, A. Harata, and T. Sawada, *Phys. Rev. B*, **58**, 8428 (1998).

17 D. W. Lynch and W. R. Hunter, "Handbook of Optical Constants of Solids," Academic Press, Boston (1991), p. 286.

18 A. Harata, Q. Shen, T. Tanaka, and T. Sawada, *Jpn. J. Appl. Phys.*, **32**, 3633 (1993).

19 Z. Shi, S. Wu, and J. Lipkowski, *J. Electroanal. Chem.*, **384**, 171 (1995).

20 Z. Shi and J. Lipkowski, *J. Electroanal. Chem.*, **403**, 225 (1996).

21 A. Kolics, A. E. Thomas, and A. Wieckowski, *J. Chem. Soc., Faraday Trans.*, **92**, 3727 (1996).

22 W. Schmickler, *Chem. Rev.*, **96**, 3177 (1996).

23 T. E. Furtak, *Surf. Sci.*, **299/300**, 945 (1994).

24 S. Cummings, J. E. Enderby, G. W. Neilson, J. R. Neusome, R. A. Howe, W. S. Howells, and A. K. Soper, *Nature*, **287**, 714 (1980).

25 C. K. Sun, F. Vallee, L. Acioli, E. P. Ippen, and J. G. Fujimoto, *Phys. Rev. B*, **48**, 12365 (1993).